scientific reports

Check for updates

OPEN

Impact of four-dimensional computed tomography phase number on target coverage of four-dimensional robustly optimized lung stereotactic body radiotherapy

Takayuki Yagihashi[1,2], Tatsuya Inoue[1,3]✉, Masashi Yamanaka[1], Shintaro Shiba[4], Akihiro Yamano[1], Naoki Sato[1], Yumiko Minagawa[4] & Motoko Omura[4]

This study evaluated the dosimetric benefits of various four-dimensional (4D) robust optimization strategies for enhancing plan robustness in free-breathing stereotactic body radiotherapy (SBRT). For ten early-stage lung cancer patients, we generated four helical tomotherapy–SBRT plans (42 Gy/4 fractions) using 4D robust optimization based on 4D-computed tomography (CT) images from all ten phases (4D_10), six phases (4D_6), four phases (4D_4), and two phases (4D_2). Conventional internal target volume (ITV)–based plans served as a reference. Setup uncertainty robustness was assessed across all CT phases. We compared dose and target coverage ($D_{98\%}$, $V_{100\%}$) for the gross tumor volume, doses to relevant organs at risk (OARs), and reductions in plan robustness for both nominal and perturbed scenarios. Optimization durations were recorded. All nominal plans met clinical criteria for targets and OARs. The 4D_10 plans exhibited the highest robustness in target coverage, with $D_{98\%}$ significantly different from ITV plans ($p < 0.05$) and $V_{100\%}$ significantly different from 4D_2 plans ($p < 0.05$). Optimization time increased linearly with the number of CT phases. Four-dimensional robust optimization enables free-breathing SBRT plans resilient to respiratory and setup uncertainties; however, limiting phase number may compromise robustness for certain tumors despite shorter optimization times.

Keywords 4D robust optimization, Free-breathing radiotherapy, Lung cancer, Lung stereotactic body radiotherapy, RayStation, Tomotherapy

Abbreviations

4D-CT	Four-dimensional computed tomography
4D_10N	Robustly optimized nominal plan with all ten phases of 4D-CT
4D_6N	Robustly optimized nominal plan with six phases of 4D-CT
4D_4N	Robustly optimized nominal plan with four phases of 4D-CT
4D_2N	Robustly optimized nominal plan with maximum expiratory and inspiratory phases of 4D-CT
4D_10P	Perturbed 4D_10N plan with consideration of the setup uncertainty
4D_6P	Perturbed 4D_6N plan with consideration of the setup uncertainty
4D_4P	Perturbed 4D_4N plan with consideration of the setup uncertainty
4D_2P	Perturbed 4D_2N plan with consideration of the setup uncertainty
GTV	Gross tumor volume

[1]Department of Medical Physics, Shonan Kamakura General Hospital, 1370-1 Okamoto, Kamakura, Kanagawa 247-8533, Japan. [2]Department of Radiological Sciences, Graduate School of Human Health Sciences, Tokyo Metropolitan University, 7-2-10 Arakawa-Ku, Tokyo 116-8551, Japan. [3]Department of Radiation Oncology, Juntendo University, 2-1-1 Hongo, Bunkyo-Ku, Tokyo 113-8421, Japan. [4]Department of Radiation Oncology, Shonan Kamakura General Hospital, 1370-1 Okamoto, Kamakura, Kanagawa 247-8533, Japan. ✉email: ttinoue@juntendo.ac.jp

ITV	Internal target volume
NSCLC	Non-small cell lung cancer
OAR	Organ at risk
PTV	Planning target volume
SBRT	Stereotactic body radiotherapy
3D_N	Nominal plan optimized using internal target volume
3D_P	Perturbed 3D_N plan with consideration of the setup uncertainty

Stereotactic body radiotherapy (SBRT) has become the standard treatment for patients with medically inoperable early-stage non-small cell lung cancer (NSCLC)[1,2]. Compared to conventional fractionated radiotherapy, SBRT enables the delivery of higher doses to a tumor in a few fractions, resulting in an excellent clinical outcome comparable to that of surgery. However, the increasing prescription dose per fraction of the hypofractionation scheme increases the risk of radiation-induced toxicities, such as pneumonitis and vascular injury, and is of concern[2,3]. In addition, patient respiration during lung radiotherapy can cause tumor movement. If unfavorable events, such as interplay effects between the moving tumor and dynamic radiation beams, cause underdosing of the tumor, the negative impact on local tumor control can be large because of the reduced averaging effect by a few treatment fractions[4]. Therefore, high-precision dose prescription methods are necessary to avoid unfavorable complications and control uncertainties associated with lung SBRT.

Robust optimization was originally developed for proton therapy treatment planning to reduce the impact of setup and range uncertainties on the dose distribution[5]. The algorithm considers uncertainty scenarios based on predefined parameters for setup error and range uncertainty during optimization and creates a dose distribution while achieving dose objectives under all uncertainty scenarios. Previously, our group demonstrated that robust optimization could compensate for the impact of setup uncertainty and intrafractional changes on dose distribution and maintain the plan robustness for target coverage while sparing the organ at risk (OAR) doses[6,7]. However, the effectiveness of robust optimization methods in mitigating the impact of tumor motion on lung cancer therapy remains limited. Subsequently, a four-dimensional (4D) robust optimization strategy was proposed to explicitly account for respiratory motion, in addition to setup and range uncertainties[8]. The algorithm directly incorporates all-phase 4D-CT images into the optimization process and considers uncertainty scenarios, including respiratory motion-induced uncertainty. Previous studies have demonstrated the effectiveness of 4D robust optimization for proton therapy through its improvement of plan robustness related to target coverage in lung cancer treatment relative to three-dimensional robust optimization[8–12]. However, manually contouring the regions of interest and dose calculation for 4D robust optimization can take a considerable amount of time because of the introduction of multiple CT images. In robust optimization for proton therapy, several researchers have investigated the effectiveness of using a limited number of CT phases to reduce the time required for optimization in routine clinical practice[13]. These studies demonstrated that selecting specific CT phases can achieve plan quality comparable to that obtained using all CT phases[11,14,15]. In contrast, the clinical role and effectiveness of robust optimization in photon therapy remain relatively undefined and exploratory, especially for SBRT. These disadvantages make the application of 4D robust optimization to photon therapy challenging. Optimizing the use of 4D robust optimization has the potential to facilitate the widespread adoption of this advanced technique. For example, determining patient-specific limited utilization numbers of 4D-CT images may reduce computational cost while maintaining plan quality. In this study, we investigated the dosimetric effects of a 4D robust optimization strategy for a cohort of patients with early-stage NSCLC by changing the utilization number of phase CT scans and its impact on the delivered dose distributions for lung SBRT. The setup errors and intrafractional changes were considered during the analysis.

Results

Figure 1 shows the boxplots of $D_{98\%}$ and $V_{100\%}$ of the gross tumor volumes (GTVs) for all ten phases of the nominal and perturbed plans. Supplementary Tables S1 and S2 summarize the patient-specific median, minimum, and maximum values for the $D_{98\%}$ and $V_{100\%}$ of the GTVs for all ten phases of the nominal and perturbed plans. All nominal plans achieved a target coverage of 100% and a dose prescription of 42 Gy for the GTVs over all ten phases. However, clinical significance was observed in the worst-case scenario for the 4D_6P, 4D_4P, and 4D_2P plans for patient Pt03, where the GTV $V_{100\%}$ was < 95%. Furthermore, the near-minimum dose of $D_{98\%}$ for the GTV was reduced by 36.8 Gy in the worst-case 4D_2P plan for patient Pt03. Table 1 summarizes the statistical values of the differences in the dosimetric parameters $D_{98\%}$ and $V_{100\%}$ for the GTVs of all breathing phases between each nominal/perturbed plan.

Figure 2 shows the boxplots of the OAR doses in the reference phase for each nominal plan. All plans achieved the clinical goals for the OARs. Supplementary Table S3 summarizes the patient-specific OAR doses. No significant differences were found in the dosimetric parameters of OARs among the nominal plans.

Supplementary Table S4 summarizes the patient-specific mean deterioration rates of GTV $D_{98\%}$ and GTV $V_{100\%}$ between the nominal plans and each worst-case perturbed plan for each respiratory phase. The median values (minimum–maximum values) of the $D_{98\%}$ in the 4D_10, 4D_6, 4D_4, 4D_2, and 3D plans were 8.1% (6.2–13.4%), 8.3% (6.2–11.9%), 8.3% (6.9–12.8%), 9.1% (6.7–12.8%), and 10.3% (7.6–13.8%), respectively. The values for the GTV $V_{100\%}$ in the 4D_10, 4D_6, 4D_4, 4D_2, and 3D plans were 0.4% (0–0.8%), 0.5% (0.1–1.3%), 0.4% (0.1–1.2%), 0.8% (0.1–1.7%), and 0.4% (0.1–0.6%), respectively.

Figure 3 presents regression analyses of mean deterioration rates of GTV $D_{98\%}$ and $V_{100\%}$ versus target amplitude and volume for ten patients. As target amplitude increased, robustness of $D_{98\%}$ and $V_{100\%}$ improved in the 4D_10, 4D_6, and 4D_4 plans but declined in the 4D_2 and ITV-based (3D) plans. Conversely, smaller tumor volumes correlated with greater robustness in the 4D-optimized plans, whereas larger volumes favored robustness in the 3D plans. Table 2 summarizes mean deterioration rates by tumor location: $D_{98\%}$ deterioration

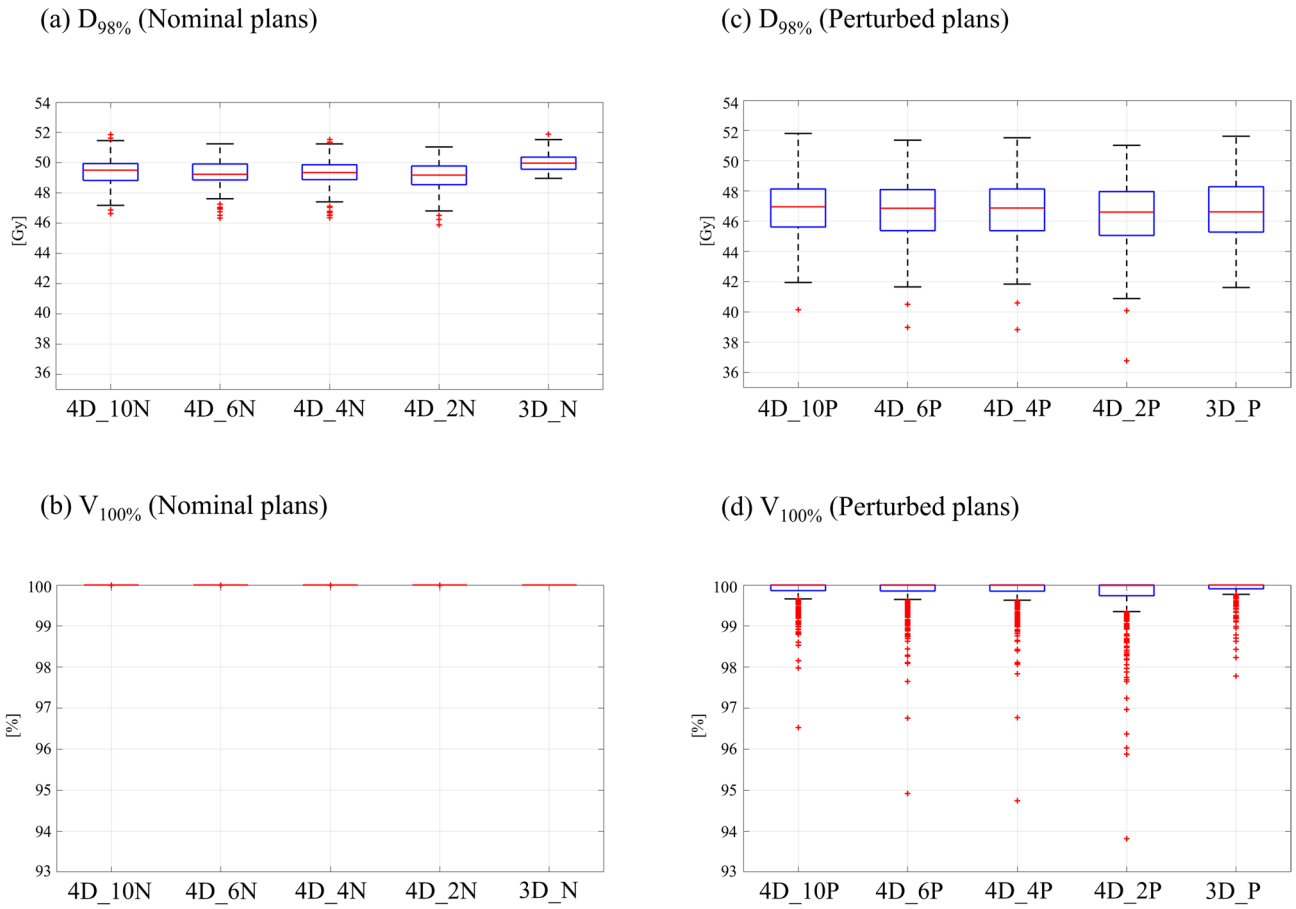

Fig. 1. Box and whisker plots illustrating the $D_{98\%}$ and $V_{100\%}$ for the GTV of the 4D robustly optimized and internal target volume-based 3D plans. (**a**) $D_{98\%}$ for nominal plans, (**b**) $V_{100\%}$ for nominal plans, (**c**) $D_{98\%}$ for perturbed dose plans considering setup uncertainty, and (**d**) $V_{100\%}$ for perturbed dose plans considering setup uncertainty.

Comparison plan A with plan B		Nominal plans		Perturbed plans		Deterioration Rate	
A	B	$D_{98\%}$	$V_{100\%}$	$D_{98\%}$	$V_{100\%}$	$D_{98\%}$	$V_{100\%}$
4D_10	4D_6	0.006	0.019				
4D_10	4D_4	0.009		0.024			
4D_10	4D_2	< 0.001		< 0.001	< 0.001		< 0.001
4D_10	3D			0.001		< 0.001	
4D_6	4D_4						
4D_6	4D_2			< 0.001	< 0.001	< 0.001	< 0.001
4D_6	3D	< 0.001	0.003		< 0.001	< 0.001	< 0.001
4D_4	4D_2	0.042		< 0.001	< 0.001	0.003	< 0.001
4D_4	3D	< 0.001			0.008	< 0.001	0.009
4D_2	3D	< 0.001		< 0.001	< 0.001	< 0.001	< 0.001

Table 1. Statistical values of the differences in the dosimetric parameters $D_{98\%}$ and $V_{100\%}$ for the gross tumor volumes of all breathing phases between each nominal plan/perturbed plan/deterioration rate.

was higher for lower-lobe tumors across all plan types, while $V_{100\%}$ deterioration remained comparable among plans except for the 4D_2 plan.

Table 3 shows the duration of optimization for each nominal plan and the ratios of the optimization durations of the 4D_6N, 4D_4N, 4D_2N, and 3D plans to the optimization duration of the 4D_10N plans for each patient. The ranges of the ratios were 0.56–0.65, 0.37–0.43, 0.19–0.23, and 0.02–0.03 for the 4D_6N, 4D_4N, 4D_2N,

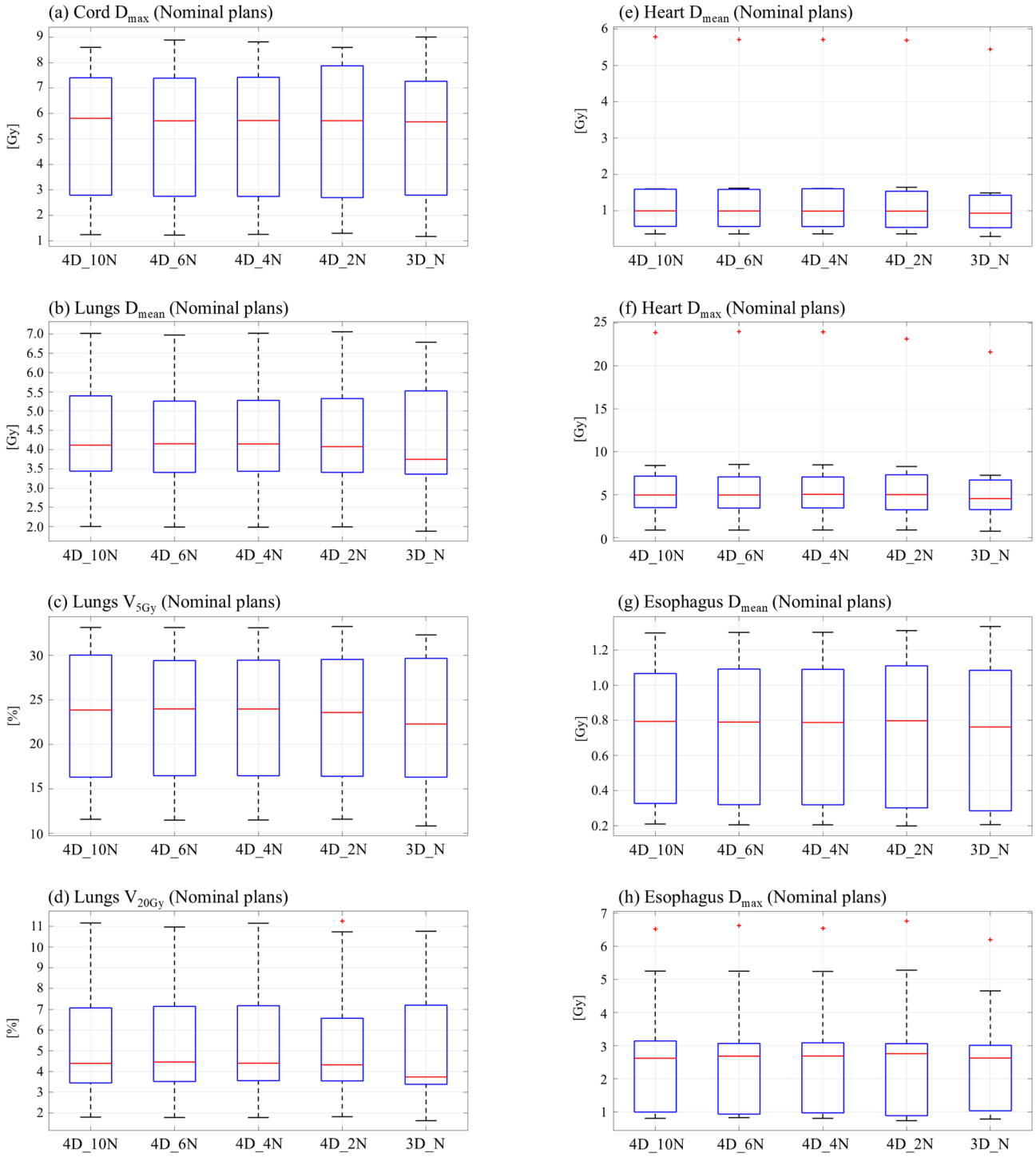

Fig. 2. Box and whisker plots showing (**a**) the maximum dose to the spinal cord; (**b**) mean dose to the lungs; (**c**) lungs V5Gy; (**d**) lungs V20Gy; (**e**) mean and (**f**) maximum dose to the heart; and (**g**) mean and (**h**) maximum doses to the esophagus for the 4D robustly optimized and internal target volume-based 3D nominal plans.

and 3D plans, respectively. For 4D robustly optimized plans, the duration was approximately proportional to the number of CT phases utilized during robust optimization. While the time for 3D plans was short by 50 times compared with that for 4D_10 plans.

Discussion

This study evaluated the dosimetric potential of 4D robust optimization for maintaining the robustness of the target dose coverage for free-breathing lung SBRT using a helical tomotherapy technique. To safely and precisely

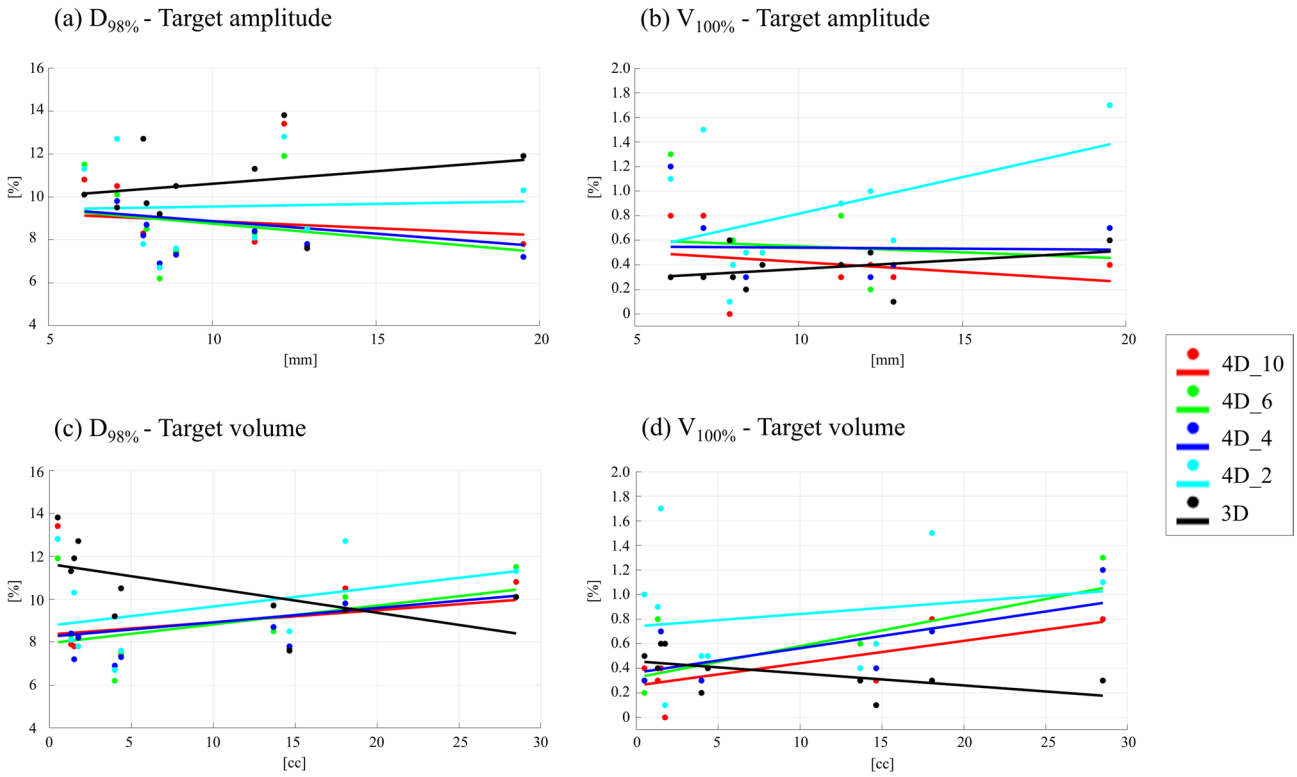

Fig. 3. Regression lines for the relationship between mean deterioration rates of GTV $D_{98\%}$ / GTV $V_{100\%}$ and patient-specific factors for the 4D robustly optimized and internal target volume-based 3D plans. (**a**) $D_{98\%}$ for target amplitude, (**b**) $V_{100\%}$ for target amplitude, (**c**) $D_{98\%}$ for target volume, (**d**) $V_{100\%}$ for target volume.

$D_{98\%}$ [%]					
	4D_10	**4D_6**	**4D_4**	**4D_2**	**3D**
Upper	8.1 ± 0.4	8.2 ± 0.3	8.3 ± 0.4	8.5 ± 0.8	10.3 ± 2.2
Lower	9.4 ± 2.7	9.1 ± 2.4	9.2 ± 2.5	10.2 ± 2.6	10.8 ± 1.7
$V_{100\%}$ [%]					
	4D_10	**4D_6**	**4D_4**	**4D_2**	**3D**
Upper	0.3 ± 0.2	0.5 ± 0.3	0.5 ± 0.3	0.5 ± 0.3	0.4 ± 0.2
Lower	0.5 ± 0.2	0.6 ± 0.4	0.6 ± 0.3	1.1 ± 0.5	0.4 ± 0.1

Table 2. Mean and standard deviation deterioration rates of $D_{98\%}$ and $V_{100\%}$ for gross tumor volumes in upper versus lower lobes, comparing 4D robustly optimized and internal target volume-based 3D plans.

perform SBRT for lung tumors, the effects of patient respiration should be controlled[16]. The most typical technique to compensate for respiratory-induced tumor motion is the use of 4D-CT images with an ITV or a mid-ventilation concept[17,18]. The ITV is generated by summing GTVs from all respiratory phases of the 4D-CT dataset. An ITV-based plan can accommodate tumor motion during free breathing but is typically created on a single CT phase (e.g., end-expiration). In contrast, 4D robust optimization incorporates multiple CT phases to capture both patient anatomy and temporal information. Consequently, 4D robust optimization more effectively manages respiratory-induced dose uncertainties, as demonstrated in previous studies[9,11]. In addition, a previous study has reported that 4D robust optimization is expected to have superior robustness for respiratory motion and intrafractional changes relative to the traditional optimization method on an average CT using an ITV[19].

In this study, $D_{98\%}$ and $V_{100\%}$ of the nominal plans achieved the clinical goal ($D_{98\%}$ > the prescription dose, $V_{100\%}$ > 95%) for GTVs for all respiratory phases for all patients. When considering setup uncertainty, differences in robustness were observed among the five optimization strategies. Overall, the robustness of the 4D_10 plans was higher than that of the other plans. When focusing on patient-wise robustness of target coverage, the worst case was observed in patient Pt03. The worst $D_{98\%}$ and $V_{100\%}$ for the 4D_6P, 4D_4P, and 4D_2P plans were < 40 Gy and < 95%, respectively, while those for the 4D_10 plans were 43.4 Gy and 98.8%, respectively. This patient had a larger tumor amplitude (11.3 mm) and smaller tumor volume (1.3 cc). Furthermore, the tumor was located at the center of the lung and not near the chest wall or mediastinum. In the case, using more CT scans should be considered to create more robust plans before treatment planning, although using a few phase CT scans leads to

		Patient									
Plan	**Time**	**Pt01**	**Pt02**	**Pt03**	**Pt04**	**Pt05**	**Pt06**	**Pt07**	**Pt08**	**Pt09**	**Pt10**
4D_10	[s]	4631	11,288	6035	8002	7083	8384	7753	5498	9387	10,094
	Ratio	–	–	–	–	–	–	–	–	–	–
4D_6	[s]	2721	6814	3437	4742	4302	4688	4526	3559	5545	6017
	Ratio	0.59	0.60	0.57	0.59	0.61	0.56	0.58	0.65	0.59	0.60
4D_4	[s]	1696	4476	2387	3160	2969	3537	2931	2172	3816	4293
	Ratio	0.37	0.40	0.40	0.39	0.42	0.42	0.38	0.40	0.41	0.43
4D_2	[s]	1005	2347	1157	1670	1557	1814	1581	1194	1980	2288
	Ratio	0.22	0.21	0.19	0.21	0.22	0.22	0.20	0.22	0.21	0.23
3D	[s]	91	262	115	134	135	153	132	175	188	180
	Ratio	0.02	0.02	0.02	0.02	0.02	0.02	0.02	0.03	0.02	0.02
		Patient									
Plan	**Time**	**Pt01**	**Pt02**	**Pt03**	**Pt04**	**Pt05**	**Pt06**	**Pt07**	**Pt08**	**Pt09**	**Pt10**
4D_10	[m]	77	188	101	133	118	140	129	92	156	168
	Ratio	–	–	–	–	–	–	–	–	-	–
4D_6	[m]	45	114	57	79	72	78	75	59	92	100
	Ratio	0.59	0.60	0.57	0.59	0.61	0.56	0.58	0.65	0.59	0.60
4D_4	[m]	28	75	40	53	49	59	49	36	64	72
	Ratio	0.37	0.40	0.40	0.39	0.42	0.42	0.38	0.40	0.41	0.43
4D_2	[m]	17	39	19	28	26	30	26	20	33	38
	Ratio	0.22	0.21	0.19	0.21	0.22	0.22	0.20	0.22	0.21	0.23
3D	[m]	2	4	2	2	2	3	2	3	3	3
	Ratio	0.02	0.02	0.02	0.02	0.02	0.02	0.02	0.03	0.02	0.02

Table 3. Optimization durations and ratios for each 4D robustly optimized and internal target volume-based 3D plan.

a considerably shorter duration of optimization. However, except for the case, no clinically relevant differences were observed among all plans (of note, this does not indicate that CT phases should be reduced without much consideration, although fewer phases lead to the considerable reduction of optimization duration).

The worst differences in the deterioration of $D_{98\%}$ and $V_{100\%}$ between the 4D_10 and 4D_2 plans were observed in patient Pt04. This patient had the largest tumor amplitude (19.5 mm) and smaller tumor volume (1.5 cc). The tumor location was the same as that observed in patient Pt03. A previous study demonstrated that 4D robust optimization can effectively compensate for respiration-induced dose uncertainty in patients with lung cancer with a larger tumor amplitude of 5 mm[11]. However, our results indicate that comprehensive factors, including large breathing amplitude, small tumor volume, and tumor location surrounding low-density tissues, may cause the lower effectiveness of 4D robust optimization. These factors are known to reduce treatment plan quality in terms of the robustness of target coverage[11,20,21]. Therefore, we explored the relationships between plan robustness and these factors. Briefly, for all plans, $D_{98\%}$ robustness was greater for upper-lobe tumors than for lower-lobe tumors, a trend observed with both 4D robust optimization and ITV strategies. Regarding tumor amplitude, 4D robust optimization using more than four CT phases maintained robustness for larger amplitudes, whereas the ITV method's robustness declined as amplitude increased. Additionally, 4D robust strategies preserved dose-coverage robustness in small tumors, while ITV plans were more robust for large volumes. These findings highlight how tumor characteristics influence the comparative performance of 4D robust optimization versus ITV strategies.

A limitation of the current study is that the dosimetric impact of 4D robust optimization was retrospectively evaluated under static free-breathing conditions using planning 4D-CT images. In clinical practice, patients frequently experience irregular respiration and baseline shifts, which can considerably affect the robustness of the target dose coverage[22,23]. Furthermore, we evaluated target robustness by calculating the doses on each CT phase in this study. However, this idealized approach did not simulate the interplay effect. In helical tomotherapy, fan-beam elements with small width longitudinally deliver to the targets during treatment, resulting in averaging out the dose deviation over multiple breathing phases. Therefore, previous studies concluded that interplay of breathing and tomotherapy delivery motions does not affect considerably plan delivery accuracy and clinically significant[24,25]. However, these studies focused on the patients or a phantom with a regular and a reproducible breathing pattern. Investigation of interplay effects for patients with irregularly breathing pattern could still be challenging. Other previous studies have calculated dose distributions that account for the interplay effect in helical tomotherapy using in-house tools, which enable dose calculations for each CT phase with phase-specific beam sinograms[26,27]. To accurately determine the efficacy of the optimization method, dosimetric studies that consider more realistic conditions using these tools or log files of patient respiration patterns and 4D-cone beam CT images acquired during treatment should be conducted[11,28]. We explored how deterioration in target robustness relates to patient-specific factors, such as tumor amplitude, volume, and location. However, the small

sample size limits the generalizability of these trends. In addition, this study focused on helical tomotherapy for SBRT. Compared with conventional volumetric-modulated arc therapy, tomotherapy has a long delivery time due to its slice-by-slice irradiation mechanism. Generally, the interplay effect adversely impacts target dose coverage not only with short breathing periods, large breathing amplitudes, small tumor volumes, and few treatment fractions, but also with long treatment times. These factors may lead to differing dosimetric outcomes between the two modalities[29]. Finally, we selected a 5 mm setup uncertainty for both robust optimization and evaluation. The appropriateness of this margin for assessing lung SBRT plan robustness warrants careful consideration, as varying the setup can affect robustness. Although motion management typically limits target motion to less than 5 mm, a 5-mm margin may not fully preserve target coverage against motion uncertainty[30]. Therefore, a comprehensive study with more diverse patients is necessary to further elucidate the aforementioned issues and reinforce the findings of this study.

In conclusion, the 4D robust optimization plans were sufficiently robust for the target dose coverage for lung SBRT with helical tomotherapy under free-breathing conditions and setup uncertainty. However, the robustness could be affected by the tumor characteristics of the patients, such as amplitude, volume, and location. Utilizing the appropriate number of CT phases during the robust optimization may compensate for the robustness of the plan.

Methods

Patient cohort and contouring

Ten patients with clinically diagnosed stage IA NSCLC (cT1N0M0 per UICC 9th Edition) between March 2021 and September 2023 who underwent planning 4D-CT scanning were included in this study. Patients were deemed medically inoperable by multidisciplinary evaluation or operable but elected SBRT after declining surgery. The median age was 81 years (range, 64–95); six were male and four were female. This study was approved by the Institutional Review Board of Tokushukai Group Ethics Committee (No.2291/September 19, 2023). All methods were performed in accordance with the relevant guidelines and regulations. The review board of Tokushukai Group Ethics Committee waived the need for informed consent by offering an opt-out option on the institution's homepage due to its retrospective nature (Tokushukai Group Ethics Committee, https://www.mirai-iryo.com/service/index.php#s03). CT was performed using a 20-row scanner (SOMATOM Definition AS Open; Siemens AG, Munich, Germany). Each 4D-CT image was reconstructed into ten phases (0–90%), with 0% and 50% representing the end-inspiration and end-expiration phases, respectively (Fig. 4a), using a respiratory management system (ANZAI belt; Anzai Medical Co., Ltd., Tokyo, Japan). The reconstruction resolution was $0.98 \times 0.98 \times 2$ mm. Experienced radiation oncologists contoured the GTVs on the 4D-CT images across all breathing phases in the RayStation Treatment Planning System owned by our institution (version 10A; RaySearch Laboratories, Stockholm, Sweden). The RayStation was installed on a local Windows workstation with an Intel Xeon CPU and NVIDIA RTX A5000 GPU. Relevant OARs, including the lungs, spinal cord, heart, and esophagus, were delineated on the end-expiration phase CT, which served as the reference CT. A deformable image registration employing an anatomically constrained deformation algorithm was applied between the reference phase CT (end-expiration, 0%) and the 4D-CTs of other phases. Consequently, all OARs on the reference CT were expanded to the other phases, and the radiation oncologists modified the contouring if needed. Table 4 summarizes the locations, volumes, and motion amplitudes of the tumors in enrolled patients. Figure 4b shows the tumor volumes and locations in the axial plane for the ten patients.

Four-dimensional robustly optimized treatment planning

For all patients, SBRT plans with the helical tomotherapy technique were created using photon energy of 6 MV, a field width of 2.5 cm, a pitch of 0.108, and a delivery time factor of 1.3[31] and a collapsed cone convolution dose engine with a dose grid size of 1 mm in the RayStation. A nominal dose of 42 Gy in four fractions was prescribed to the GTV[32]. Four 4D robust optimization strategies were assessed using different CT phase sets for treatment planning: (1) all ten 4D-CT phases; (2) six phases (20%, 30%, 70%, 80%, end-expiration, and end-inspiration) (3) four phases (30%, 80%, end-expiration, and end-inspiration) (4) two phases (end-expiration and end-inspiration). This phase selection was based on a previous study[32] and our assumption that the two extreme phases plus representative mid-phases adequately capture target motion. Each plan was optimized by minimizing the worst-case scenario dose distribution across the specified 4D-CT phases, targeting robust GTV coverage against a setup uncertainty of 5 mm in six directions: left, right, anterior, posterior, superior, and inferior. The optimization problems were identical for all plans, with the goal of 100% of the GTV receiving at least 48 Gy. OARs, such as normal lung, spinal cord, heart, and esophagus, were included in the 4D optimization. Dose constraints followed a previous recommendation[32]: lung $V_{15Gy} < 25\%$, lung $V_{20Gy} < 20\%$, lung $D_{mean} < 18$ Gy, spinal cord $D_{max} < 25$ Gy, heart $D_{15cc} < 30$ Gy, esophagus $D_{1cc} < 40$ Gy, and $D_{10cc} < 35$ Gy. To maximize OAR sparing without compromising target coverage, we adjusted dose objectives and weights while keeping parameters identical for each patient. Notably, the robust objective was applied only to the GTV; no specific constraints were imposed on OARs in this study. All plans were normalized after optimization, and 100% of the GTVs received 130% of the prescription dose. These plans are referred to as the nominal plans for (1) 4D_10N, (2) 4D_6N, (3) 4D_4N, and (4) 4D_2N. For the 4D_6N, 4D_4N, and 4D_2N plans, the nominal plans were recalculated for the unutilized phase CTs during the robust optimization to evaluate the dosimetric parameters for all-phase CTs. Figure 5a and b show the representative dose distributions of the four nominal plans and the different dose distributions between the 4D_10N and 4D_2N plans on the end-expiration phase CT in the coronal direction (patient Pt03).

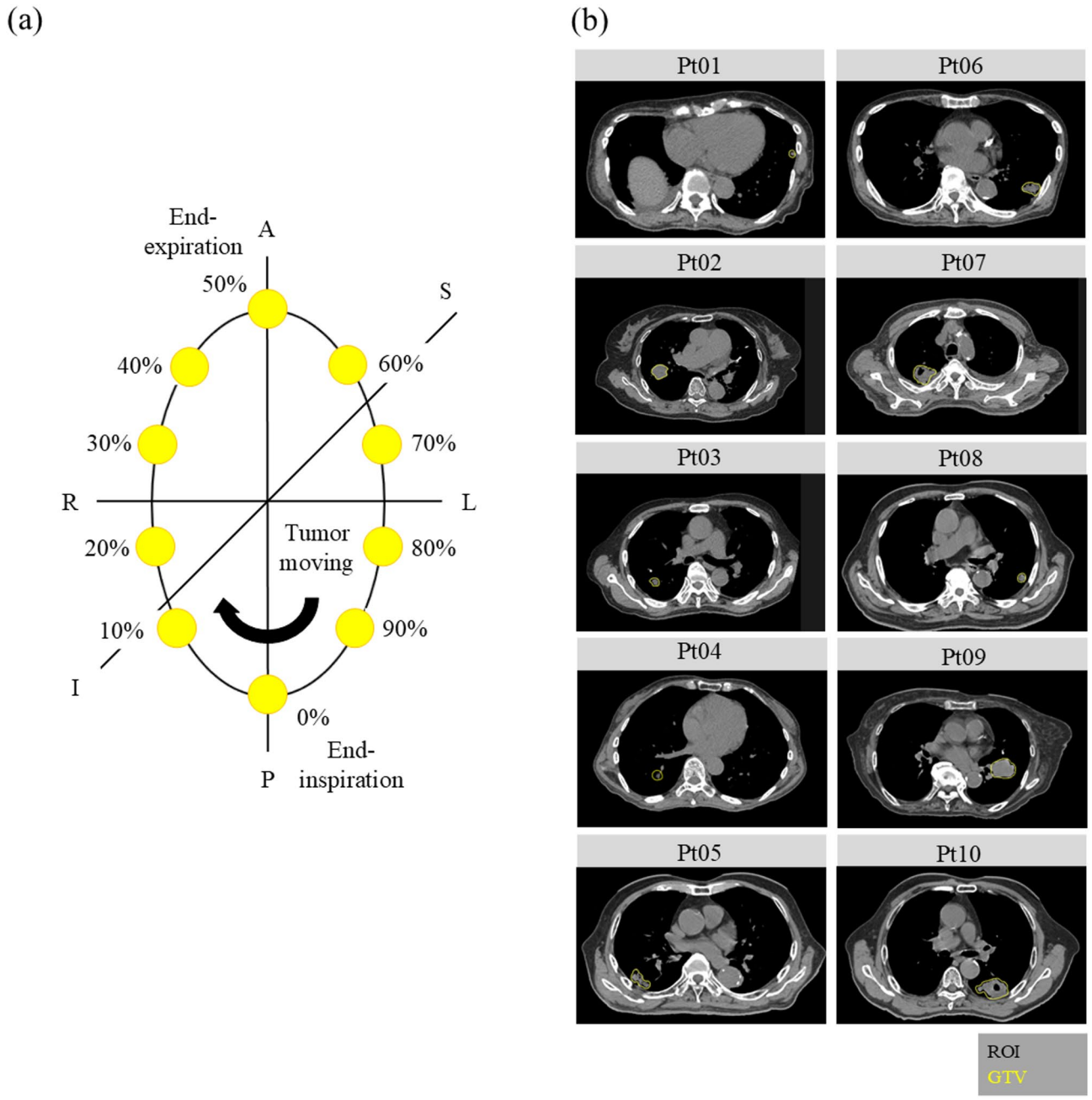

Fig. 4. Schematic view of respiratory phase and representative CT images. (**a**) Correspondence diagram for the respiration phase of 4D-CT. (**b**) Axial plane image of the maximum exhale phase in 4D-CT for 10 patients, showing lung tumors (gross tumor volume) delineated in yellow. GTV, gross tumor volume; ROI, region of interest.

Internal target volume-based treatment planning

As a reference, we also created conventional ITV–based treatment plans for the same ten patients. We defined the planning target volume (PTV) by summing GTVs across all breathing phases (the ITV) and adding a 5 mm margin in all directions. After mapping the PTV onto the maximum exhale CT phase (50%), plans were optimized to deliver 42 Gy covering ≥ 95% of the PTV while limiting hot spots to < 130% of the prescription dose. To ensure a fair comparison, planning and optimization parameters, except for the target definition, were identical between the 4D robust optimization plans and the ITV-based plans. These ITV-based plans are hereafter referred to as 3D plans.

Simulation of setup uncertainty

Perturbed dose plans considering the setup uncertainty scenarios were created by shifting the isocenter of the nominal plan by 5 mm in six directions on all 4D-CT phases. This was followed by recalculation of the

Patient ID	Age	Gender	Tumor location	GTV volume on maximum exhale CT [cc]	GTV amplitude between maximum exhale and maximum inhale CTs [mm]
Pt01	75	Female	LLL	0.5	12.2
Pt02	86	Female	RUL	14.7	12.9
Pt03	81	Male	RUL	1.3	11.3
Pt04	64	Female	RLL	1.5	19.5
Pt05	88	Male	RLL	4.4	8.9
Pt06	95	Male	LLL	4.0	8.4
Pt07	78	Male	RUL	13.7	8.0
Pt08	81	Male	LUL	1.8	7.9
Pt09	85	Female	LLL	18.1	7.1
Pt10	76	Male	LLL	28.5	6.1

Table 4. Tumor characteristics including age, gender, location, volume, and motion amplitude. GTV, gross tumor volume; RLL, right lower lobe; RUL, right upper lobe; LLL, left lower lobe; LUL, left upper lobe.

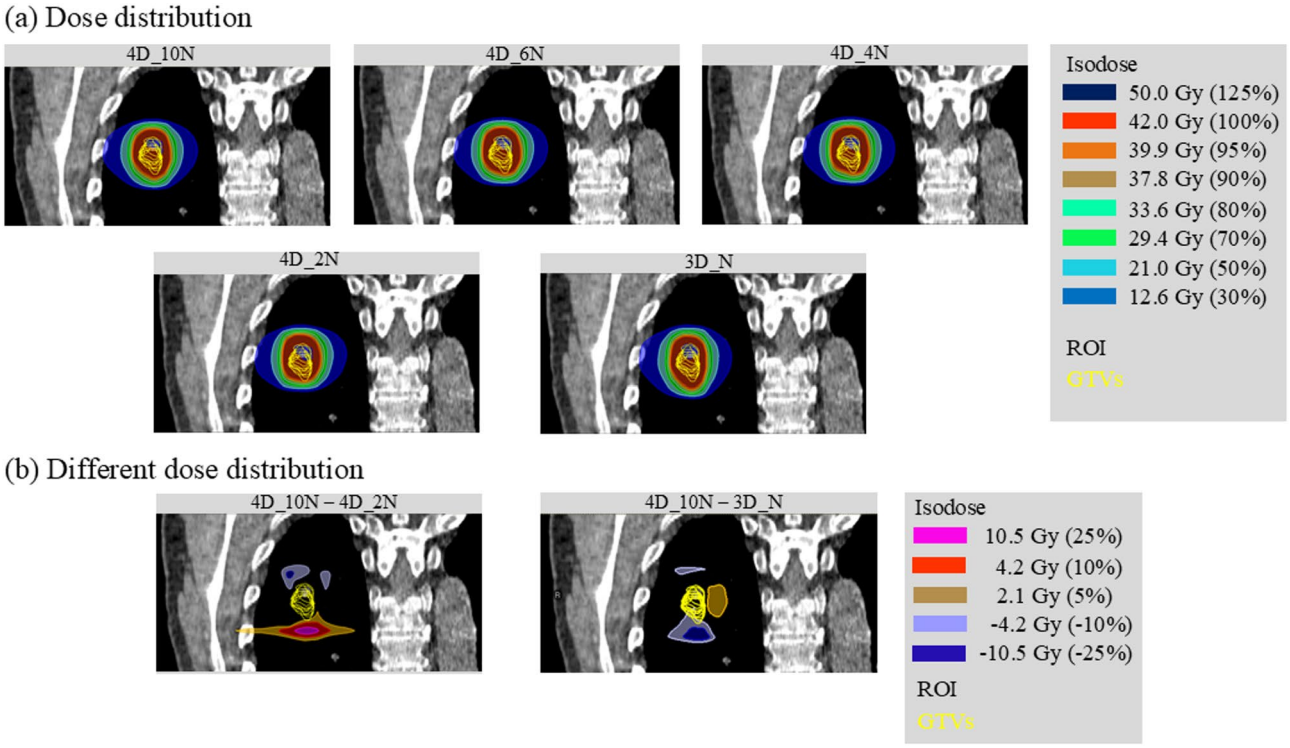

Fig. 5. Dose distributions. (**a**) Representative dose distributions for the five types of nominal plans on a coronal plane for patient Pt03. (**b**) Comparison of dose distributions between the 4D_10N and 4D_2N plans, and the 4D_10N and 3D_N plans in the coronal plane. GTV, gross tumor volume; ROI, region of interest.

dose distributions with identical plan parameters of the nominal plans. Consequently, 60 perturbed plans (ten breathing phases × six directions) were created for each 4D robust plan per patient. These plans are referred to as perturbed dose plans for (1) 4D_10P, (2) 4D_6P, (3) 4D_4P, and (4) 4D_2P.

Plan quality evaluation

Dose and target coverage, defined as the dose covering 98% of the GTV ($D_{98\%}$) and the GTV receiving the prescription dose ($V_{100\%}$), were calculated for all nominal and perturbed plans. The minimum dose $D_{98\%}$ less than the prescription dose of 95% and target coverage $V_{100\%}$ less than 95% for the GTV were defined as clinical significance. We aimed to evaluate whether treatment plans generated using 4D robust optimization can maintain target robustness across all CT phases when accounting for uncertainties. Consequently, we did not create a 4D accumulated dose via deformable image registration. Instead, we assessed dose metrics and target coverage for each CT phase in both the nominal and perturbed plans. The maximum doses for the spinal cord, heart, and esophagus; mean doses for the lungs, heart, and esophagus; and relative volumes receiving 5 and 20 Gy for the lungs were evaluated for the nominal plans. Dosimetric parameters for the OARs were calculated

only for the reference phase. For all parameters, the box and whisker plots were created, where the outliers were defined as the data exceeding the quartile range by a factor of 1.5. However, the outliers were all included in this study. Furthermore, the relationship between the tumor amplitude/tumor volume/tumor location and mean deterioration rates of $D_{98\%}$ and $V_{100\%}$ for the GTV comparing nominal plans and each worst-case perturbed plan for each phase were analyzed. In addition, the durations of optimization for each 4D robust nominal plan were recorded.

Statistical analysis

The Friedman test with Bonferroni correction was used in MATLAB (2023b, Mathworks Inc., Natick, MA, USA) for the statistical analyses of differences in the four 4D robust optimization strategies related to the target and dose coverage of the GTV and the calculation of the p-values. Statistical significance was set at $p < 0.05$.

Data availability

Data supporting the findings of this study are available from the corresponding author upon reasonable request.

Received: 6 January 2025; Accepted: 3 October 2025
Published online: 10 November 2025

References

1. Zheng, X. et al. Survival outcome after stereotactic body radiation therapy and surgery for stage I non-small cell lung cancer: A meta-analysis. *Int. J. Radiat. Oncol. Biol. Phys.* **90**, 603–611 (2014).
2. Zhang, B. et al. Matched-pair comparisons of stereotactic body radiotherapy (SBRT) versus surgery for the treatment of early stage non-small cell lung cancer: A systematic review and meta-analysis. *Radiother. Oncol.* **112**, 250–255 (2014).
3. Videtic, G. M. M. et al. Stereotactic body radiation therapy for early-stage non-small cell lung cancer: Executive summary of an ASTRO evidence-based guideline. *Pract. Radiat. Oncol.* **7**, 295–301 (2017).
4. Ali, A. M., Greenwood, J. B., Hounsell, A. & McGarry, C. A systematic review of the dosimetric consequences of the interplay effect. *Phys. Med.* **134**, 105004 (2025).
5. Fredriksson, A., Forsgren, A. & Hårdemark, B. Minimax optimization for handling range and setup uncertainties in proton therapy. *Med. Phys.* **38**, 1672–1684 (2011).
6. Yagihashi, T. et al. Comparing efficacy between robust and PTV margin-based optimizations for interfractional anatomical variations in prostate tomotherapy. *In Vivo* **38**, 409–417 (2024).
7. Yagihashi, T. et al. Effectiveness of robust optimization against geometric uncertainties in TomoHelical planning for prostate cancer. *J. Appl. Clin. Med. Phys.* **24**(4), e13881 (2023).
8. Liu, W. et al. Exploratory study of 4D versus 3D robust optimization in intensity modulated proton therapy for lung cancer. *Int. J. Radiat. Oncol. Biol. Phys.* **95**, 523–533 (2016).
9. Ribeiro, C. O. et al. Comprehensive 4D robustness evaluation for pencil beam scanned proton plans. *Radiother. Oncol.* **136**, 185–189 (2019).
10. Wang, W.-Y. et al. Comparison between 4D robust optimization methods for carbon-ion treatment planning. *Nucl. Sci. Tech.* **34**(9), 139 (2023).
11. Spautz, S. et al. Comparison of 3D and 4D robustly optimized proton treatment plans for non-small cell lung cancer patients with tumour motion amplitudes larger than 5 mm. *Phys. Imaging Radiat. Oncol.* **27**, 100465 (2023).
12. Wolf, M., Anderle, K., Durante, M. & Graeff, C. Robust treatment planning with 4D intensity modulated carbon ion therapy for multiple targets in stage IV non-small cell lung cancer. *Phys. Med. Biol.* **65**, 215012 (2020).
13. Knopf, A.-C. et al. Clinical necessity of multi-image based (4DMIB) optimization for targets affected by respiratory motion and treated with scanned particle therapy: A comprehensive review. *Radiother. Oncol.* **169**, 77–85 (2022).
14. Ma, Y. et al. Selection of breathing phase number in 4D scanned proton treatment planning optimization for lung tumors. *Phys. Med.* **114**, 103152 (2023).
15. Fan, X. et al. Effect of breathing phase number on the 4D robust optimization for pancreatic cancer intensity modulated proton therapy. *BMC Cancer* **24**(1), 1337 (2024).
16. Ball, H. J. et al. Results from the AAPM Task Group 324 respiratory motion management in radiation oncology survey. *J. Appl. Clin. Med. Phys.* **23**(11), e13810 (2022).
17. Guckenberger, M. et al. ESTRO ACROP consensus guideline on implementation and practice of stereotactic body radiotherapy for peripherally located early stage non-small cell lung cancer. *Radiother. Oncol.* **124**, 11–17 (2017).
18. Ehrbar, S. et al. ITV, mid-ventilation, gating or couch tracking: A comparison of respiratory motion-management techniques based on 4D dose calculations. *Radiother. Oncol.* **124**, 80–88 (2017).
19. Feng, H. et al. Technical Note: 4D robust optimization in small spot intensity-modulated proton therapy (IMPT) for distal esophageal carcinoma. *Med. Phys.* **48**, 4636–4647 (2021).
20. Liu, G. et al. Simulation of dosimetry impact of 4DCT uncertainty in 4D dose calculation for lung SBRT. *Radiat. Oncol.* **14**(1), 1 (2019).
21. Trémolières, P. et al. Lung stereotactic body radiation therapy: Personalized PTV margins according to tumor location and number of four-dimensional CT scans. *Radiat. Oncol.* **17**, 5 (2022).
22. Sano, K. et al. Optimal threshold of a control parameter for tomotherapy respiratory tracking: A phantom study. *J. Appl. Clin. Med. Phys.* **24**(5), e139014 (2023).
23. Tse, M. Y., Chan, W. K. C., Fok, T. C., Chiu, T. L. & Yu, S. K. Dosimetric impact of phase shifts on Radixact synchrony tracking system with patient-specific breathing patterns. *J. Appl. Clin. Med. Phys.* **23**, e13600 (2022).
24. Kissick, M. W. et al. A phantom model demonstration of tomotherapy dose painting delivery, including managed respiratory motion without motion management. *Phys. Med. Biol.* **55**, 2983–2995 (2010).
25. Sterpin, E. et al. Helical tomotherapy for SIB and hypo-fractionated treatments in lung carcinomas: A 4D Monte Carlo treatment planning study. *Radiother. Oncol.* **104**, 173–180 (2012).
26. Lu, L., Chao, E., Zhu, T., Wang, A. Z. & Lian, J. Sequential monoscopic image-guided motion compensation in tomotherapy stereotactic body radiotherapy (SBRT) for prostate cancer. *Med. Phys.* **50**, 518–528 (2023).
27. Ferris, W. S. et al. Using 4D dose accumulation to calculate organ-at-risk dose deviations from motion-synchronized liver and lung tomotherapy treatments. *J. Appl. Clin. Med. Phys.* **23**(7), e13627 (2022).
28. Ribeiro, C. O. et al. Towards the clinical implementation of intensity-modulated proton therapy for thoracic indications with moderate motion: Robust optimised plan evaluation by means of patient and machine specific information. *Radiother. Oncol.* **157**, 210–218 (2021).
29. Duan, W. et al. Dosimetric comparison of gamma knife and linear accelerator (VMAT and IMRT) plans of SBRT of Lung tumours. *Sci. Rep.* **14**(1), 22949 (2024).

30. Li, Y. et al. Using 4DCBCT simulation and guidance to evaluate inter-fractional tumor variance during SABR for lung tumor within the lower lobe. *Sci. Rep.* **11**(1), 19976 (2021).
31. Yagihashi, T. et al. Impact of delivery time factor on treatment time and plan quality in tomotherapy. *Sci. Rep.* **13**(1), 12207 (2023).
32. Kimura, T. et al. A randomized Phase III trial of comparing two dose-fractionations stereotactic body radiotherapy (SBRT) for medically inoperable stage IA non-small cell lung cancer or small lung lesions clinically diagnosed as primary lung cancer: Japan Clinical Oncology Group Study JCOG1408 (J-SBRT trial). *Jpn. J. Clin. Oncol.* (2017)

Acknowledgements
We would like to thank Editage (www.editage.jp) for English language editing.

Author contributions
Takayuki Yagihashi and Tatsuya Inoue made substantial contributions to the conception of the study. Takayuki Yagihashi, Masashi Yamanaka, Akihiro Yamano, and Naoki Sato made significant contributions to the data analysis and interpretation. Shintaro Shiba, Yumiko Minagawa, Motoko Omura, and Tatsuya Inoue made significant contributions to the design of the work and the interpretation of data. Takayuki Yagihashi and Tatsuya Inoue drafted the original manuscript. All authors critically reviewed and revised the manuscript draft and approved the final version for submission.

Funding
This work was supported by the Policy-Based Medical Services Foundation, Tokyo, Japan, Grant/Award Number: 8 in 2023, and Kazuya Yamashita Research Grant 2024 from the Japanese Society of Radiological Technology.

Declarations

Competing interests
The authors declare no competing interests.

Additional information
Supplementary Information The online version contains supplementary material available at https://doi.org/10.1038/s41598-025-23090-z.

Correspondence and requests for materials should be addressed to T.I.

Reprints and permissions information is available at www.nature.com/reprints.

Publisher's note Springer Nature remains neutral with regard to jurisdictional claims in published maps and institutional affiliations.